J. Preston, and P. A. Cruickshank [*J. Am. Chem. Soc.* **87**, 2492 (1965); W. Konig and R. Geiger, *Chem. Ber.* **103**, 788 (1970)]. The coupling was carried out in *N*,*N*-dimethylformamide (DMF) (Sigma) with addition of 5 to 10% H_2O to increase solubility of the salt and 1.2 equivalents of 1-hydroxybenzotriazole (Sigma) to reduce racemization of glutamine. The product was purified by rpHPLC (*10*) on the YMC column eluted with 25% CH_3CN in 0.4 mM ammonium acetate buffer (Aldrich) at a flow rate of 1.2 ml/min. The retention time of the synthetic and natural elicitor was identical.

24. The D- and L-glutamine forms of synthetic volicitin were separated on a 250-mm, 4.6-mm ID chirobiotic T column (Advanced Separation Technologies, Whippany, NJ) eluted with 10% CH_3CN in 10 mM ammonium acetate buffer, pH 4.5, at a flow rate of 1 ml/min (*10*). The synthetic L-form had a retention time of 5.25 min, identical to that of the natural elicitor, and the D-form had a retention time of 9.03 min.
25. E. E. Farmer and C. A. Ryan, *Plant Cell* **4**, 129 (1992).
26. R. Kramell *et al.*, *J. Plant Growth Regul.* **14**, 29 (1995).
27. K. E. Ricker and R. M. Bostock, *Physiol. Mol. Plant Pathol.* **44**, 65 (1994), and references therein.
28. J. H. Loughrin, A. Manukian, R. R. Heath, T. C. J. Turlings, J. H. Tumlinson, *Proc. Natl. Acad. Sci. U.S.A.* **91**, 11836 (1994).
29. U. S. R. Röse, A. Manukian, R. R. Heath, J. H. Tumlinson, *Plant Physiol.* **111**, 487 (1996).
30. P. W. Pare and J. H. Tumlinson, *Nature* **385**, 30 (1997).
31. T. C. J. Turlings and J. H. Tumlinson, *Proc. Natl. Acad. Sci. U.S.A.* **89**, 8399 (1992).
32. L. Mattiacci, M. Dicke, M. A. Posthumus, *ibid.* **92**, 2036 (1995).
33. Significant differences in relative release rates of volatiles were tested by Tukey's studentized range test after analysis of variance with a significance level of 5% (SYSTAT, Systat Inc., Evanston, IL).
34. This project was funded in part by a grant from the Swedish Natural Science Research Council. We thank H. Karlsson, A. T. Proveaux, and D. Powell for assistance with mass spectrometric analysis, J. Lockerman and S. Sharp for oral secretion collection, and M. Brennan for technical assistance. We also thank J. G. Millar, C. A. Ryan, and G. G. Still for helpful comments on the manuscript.

24 January 1997; accepted 17 March 1997

A Tonic Hyperpolarization Underlying Contrast Adaptation in Cat Visual Cortex

Matteo Carandini* and David Ferster

The firing rate responses of neurons in the primary visual cortex grow with stimulus contrast, the variation in the luminance of an image relative to the mean luminance. These responses, however, are reduced after a cell is exposed for prolonged periods to high-contrast visual stimuli. This phenomenon, known as contrast adaptation, occurs in the cortex and is not present at earlier stages of visual processing. To investigate the cellular mechanisms underlying cortical adaptation, intracellular recordings were performed in the visual cortex of cats, and the effects of prolonged visual stimulation were studied. Surprisingly, contrast adaptation barely affected the stimulus-driven modulations in the membrane potential of cortical cells. Moreover, it did not produce sizable changes in membrane resistance. The major effect of adaptation, evident both in the presence and in the absence of a visual stimulus, was a tonic hyperpolarization. Adaptation affects a class of synaptic inputs, most likely excitatory in nature, that exert a tonic influence on cortical cells.

Adaptation is a fundamental sensory process that allows neurons to respond with high sensitivity to a wide range of sensory inputs. One aspect of sensory stimuli to which neurons in the visual cortex adapt is contrast (*1*–*4*): Adaptation to high contrasts increases the threshold contrast required to evoke a given response, whereas adaptation to low contrasts decreases that threshold (*3*). Adaptation therefore acts as a gain control mechanism that maximizes the sensitivity of cortical cells to the average contrast of their most recent stimuli (*4*, *5*). Recent theories suggest that adaptation may have an even broader role in enhancing the coding efficiency of the cerebral cortex (*6*).

Previous studies of contrast adaptation in the visual cortex were based on extracellular measurements of spike responses. Although these measurements indicate what a cell communicates to the rest of the brain, they do not provide many clues to the cellular mechanisms underlying adaptation. To investigate these mechanisms, we made intracellular recordings from 27 neurons of the cat primary visual cortex (*7*).

Intracellular records for a cortical simple cell are shown in Fig. 1. In our sample of 15 simple cells, the spike responses to drifting gratings and their dependence on contrast were consistent with those observed in extracellular experiments: (i) The cells' firing rates (Fig. 1A) were strongly modulated by the passage of each cycle of the stimulus grating (*8*). (ii) The amplitude of this modulation, as measured by the first harmonic (F1) component of the response at the stimulus temporal frequency, grew with contrast. (iii) In all cells, the relation between stimulus contrast and the F1 component of the firing rate (Fig. 1E, solid circles) was well fit by a hyperbolic ratio (*9*),

$$R(c) = R_{max}c^n/(\sigma^n + c^n) \qquad (1)$$

where c is stimulus contrast, R is the cell's response, and R_{max}, σ, and n are free parameters.

The fluctuations in membrane potential evoked by drifting gratings were nearly sinusoidal at all contrasts (Fig. 1C, thick traces). Increasing contrast had a dual effect on the responses: It increased the amplitude of the stimulus-modulated (F1) component of the response, and it increased the mean level around which the modulation occurred (the DC component) (*10*). The dependence of both the F1 and DC components on contrast was also well fit by a hyperbolic ratio, except for a decrease at the highest contrasts observed in most of our cells (Fig. 1, D and F, solid circles).

The responses described so far were obtained while the cell was adapted to low contrasts, that is, while the seven test stimuli (1, 2, 4, 8, 16, 32, and 64% contrast) were interleaved with exposure to 1.5% contrast adapting stimuli. To change the cell's adaptation state, we alternated these low-adaptation measurements of contrast response with high-adaptation measurements in which the same seven test stimuli were interleaved with exposure to 47% contrast adapting stimuli (*3*, *11*). Consistent with previous reports (*1*–*4*), adaptation reduced the spike responses (Fig. 1B). In particular, it shifted the contrast response curve to the right (*3*, *4*) (Fig. 1E, open circles); adaptation thus decreased the sensitivity of the cell by half, so that obtaining a given response amplitude required twice the stimulus contrast.

The effect of adaptation on the membrane potential responses can be seen by comparing the thick and thin traces (1.5% and 47% contrast, respectively) in Fig. 1C. Surprisingly, the changes observed in the F1 component of the spike responses were not mirrored by changes in the size of the sinusoidal membrane potential modulation. Indeed, there was neither a rightward nor a downward shift in the contrast response curve derived from the F1 component of the membrane potential (Fig. 1D). The main effect of adaptation on the membrane potential was to shift the membrane potential down by as much as 15 mV (Fig. 1C, thin traces). This hyperpolarization was reflected in a downward shift of the contrast response curve constructed from the DC component of the membrane potential (Fig. 1F, open circles). Because of the lack of adaptation effects on the F1 component of the membrane potential, this downward shift

Department of Neurobiology and Physiology, Northwestern University, Evanston, IL 60208, USA.

*Present address: Center for Neural Science, New York University, 4 Washington Place, New York, NY 10003, USA.

must be principally responsible for the commonly observed rightward shift in the contrast response function constructed from the cell's spike responses.

In all seven simple cells tested as in Fig. 1, the effect on the F1 component of the membrane potential response was much smaller than the adaptation-induced reduction in the mean potential. The simple cell that showed the largest effect on F1 is illustrated in Fig. 2. In this cell, the modulation of the membrane potential evoked by a 16% contrast test stimulus was noticeably decreased in amplitude by adaptation (Fig. 2C). This effect is visible as a rightward shift of the corresponding contrast response curve (Fig. 2D). Even so, at all contrasts, the drop in the DC component of the membrane potential (Fig. 2F) was larger than the corresponding reduction in the amplitude of the F1 component (Fig. 2D). Overall, the F1 component of the membrane potential was remarkably invariant in the face of substantial hyperpolarization. This invariance could be ascribed to the opposite effects of hyperpolarization on the driving forces of the excitatory and inhibitory components of the response (*12*).

Adaptation effects were measured in 11 cells (9 simple and 2 complex) with a different sequence of stimuli from that used in Figs. 1 and 2, a sequence that was also used in previous extracellular experiments (*13*). The gratings were presented with an initial contrast of 1%, which was then increased in 4-s intervals to 64%. Once the contrast reached 64%, it was stepped back down to 1%. With this method, two stimuli of the same contrast, one presented on the way up and one on the way down, were preceded by different contrasts and so were presented while the cell was in different adaptation states. The results of these ramp experiments are shown for three simple cells in Fig. 3. In ramp experiments, adaptation was weaker than in experiments with interleaved adapting stimuli (Figs. 1 and 2). This difference occurred presumably because in the interleaved experiments the low- and high-contrast adapting stimuli differed in contrast by a factor of >30, much larger than the factor of 3 or 4 in ramp experiments. As in the interleaved experiments, substantial hyperpolarization was seen at contrasts that evoked little membrane potential modulation and few spikes, and adaptation induced a reduction of stimulus-evoked membrane potential modulations that was much smaller than the accompanying hyperpolarization. In the nine simple cells tested with contrast ramps, the strength of adaptation of the DC component of the membrane potential was typically

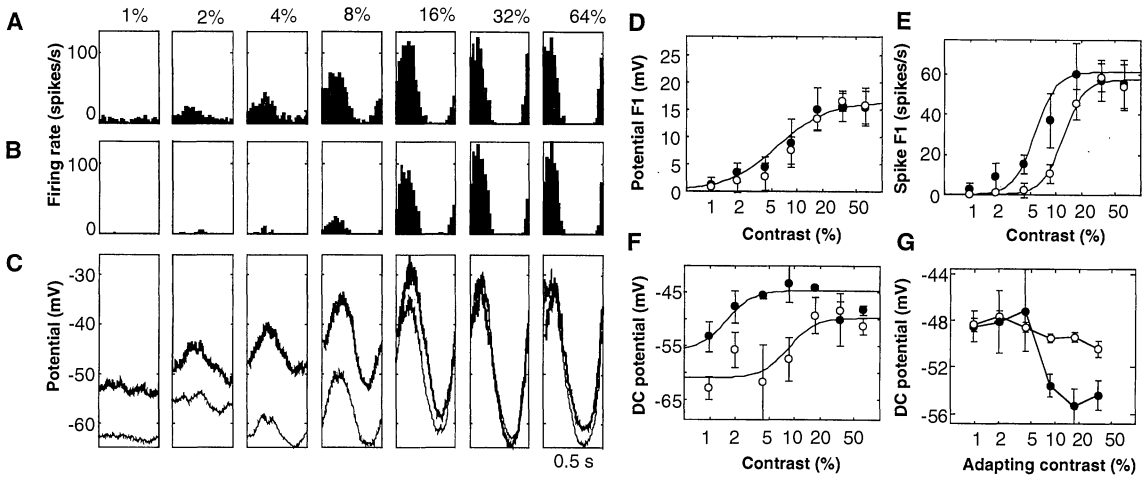

Fig. 1. Intracellularly recorded responses of a simple cell to optimal drifting gratings presented at seven different test contrasts in two different adaptation conditions. (**A** and **B**) Period histograms of the spike responses after adaptation to 1.5% and 47% contrast, respectively. (**C**) Cycle averages of the membrane potential after adaptation to 1.5% contrast (thick traces) and 47% contrast (thin traces). Each block of seven test stimuli was preceded by 20 s of an adapting stimulus, which was also presented for 4 s between each test stimulus. Test stimuli lasted 4 s, and their order of presentation was randomized within each block. Blocks with 1.5% adapting contrast were alternated with blocks with 47% adapting contrast. Each block was run three times, so the histograms and traces are averages of the responses to 24 cycles of the grating. (**D** to **F**) Contrast response curves [(D), F1 component of the membrane potential; (E), F1 component of the spike train; (F), DC component of the membrane potential] obtained after adapting to 1.5% contrast (●) and 47% contrast (○). Error bars are twice the SEM over different blocks (N = 3). Data are fitted by Eq. 1, with the exponent n constrained to be the same for the two fits in each graph. (**G**) The DC component of the membrane potential responses to 1.5% contrast (●) and 47% contrast (○) plotted against the contrast of the preceding stimulus.

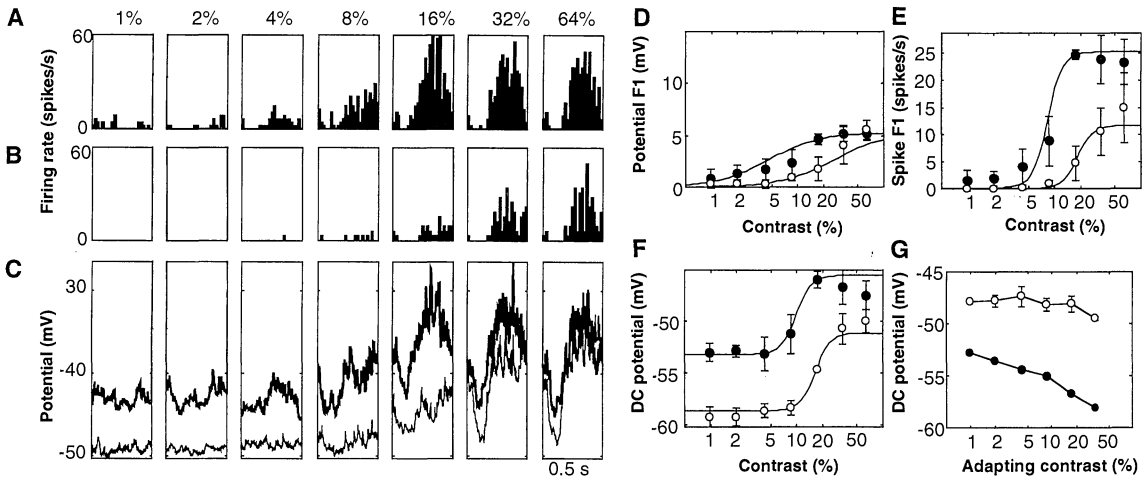

Fig. 2. Effects of contrast adaptation on a second simple cell. The layout and symbols are identical to those of Fig. 1. N = 3 for the unadapted condition and N = 2 for the adapted condition.

nine times that of the F1 component (Fig. 3).

In simple cells, adaptation-induced hyperpolarizations were larger during low-contrast stimulation than they were at high contrasts. To measure this difference explicitly, we reversed the roles assigned to the test and adapting stimuli, plotting the mean potential of the responses to the adapting stimuli as a function of the contrast of the preceding test stimulus (Figs. 1G and 2G). In the seven simple cells tested with interleaved adapting stimuli, adaptation hyperpolarized the cells by 5.1 ± 1.2 mV (mean ± SEM) at 1% test contrast and by 3.0 ± 0.4 mV at 64% test contrast. All of our adapting and test stimuli were optimal in orientation and spatial frequency. Because adaptation-induced reductions in sensitivity have been shown to be partly selective for the stimuli used to elicit them (*3*, *6*, *14*), it is likely that the effect at higher contrasts would depend on the stimulus used to test the cells. In any event, the strongest effects of adaptation that we measured in simple cells were most often observed as the contrast of the test stimulus decreased toward zero, and were thus independent of the test stimulus.

As expected from extracellular studies of the responses of complex cells to drifting gratings (*15*), we did not find a modulated (F1) component in the membrane potential responses of the 12 complex cells in our sample. As a result, only the DC responses of these cells were considered. As in simple cells, at any given adaptation state increasing the contrast of the test stimulus depolarized the cells, increasing their mean potential by 2 to 10 mV. This increase was well fitted by a hyperbolic ratio function (Eq. 1). In all but one complex cell, adaptation induced a decrease in the mean potential of up to 4 mV. Contrary to simple cells, in complex cells this decrease was weaker at low test contrasts than at high test contrasts (0.2 ± 0.6 mV at 1% test contrast, 2.7 ± 0.9 mV at 64% test contrast; $N = 10$). In addition, in 7 out of 10 complex cells, the DC potential contrast curves appeared to be shifted to the right by adaptation (not shown). This behavior would be expected if complex cells received a substantial portion of their synaptic input from simple cells, because the contrast response curves measured from the spike output of simple cells also shift to the right during adaptation.

Perhaps the simplest explanation for the effects of adaptation that we have described is that simple cells receive two classes of synaptic inputs: phasic and tonic (*16*). According to this hypothesis, phasic inputs generate the stimulus-driven modulations in membrane potential and are unaffected by adaptation; tonic inputs remain active even in the absence of visual stimulation, and their activity is affected by adaptation and produces the tonic hyperpolarization. Although the phasic inputs are known to originate from both excitatory and inhibitory neurons (*12*), we do not know whether the tonic inputs are excitatory and suppressed during adaptation or are inhibitory and enhanced during adaptation. Indeed, both excitation (*17*, *18*) and inhibition (*2*, *3*, *19*, *20*) have been proposed as possible substrates for cortical adaptation.

To distinguish between these two possibilities, we measured visually evoked changes in membrane conductance. If the adaptation-induced hyperpolarization were caused by a reduction in tonic excitation, it would be accompanied by a reduction in membrane conductance. Conversely, if the hyperpolarization were caused by an increase in tonic inhibition, it would be accompanied by an increase in membrane conductance. Because of the large difference in the driving forces on excitatory and inhibitory synaptic potentials, the withdrawal of excitation required to hyperpolarize the cell by 5 mV would produce only a small change in the cell's input resistance, whereas the required increase in inhibition would produce a large change in input resistance (*21*). To look for such changes in input resistance, we injected DC currents into cells during visual stimulation and measured the current-evoked changes in DC membrane potential. A complete experiment, repeated for two different adaptation states, included three different currents injected during visual stimulation with two different contrasts. The relation between current and voltage for each of the four combinations of visual stimulation and adaptation was described by a line, the slope of which is equal to the input resistance

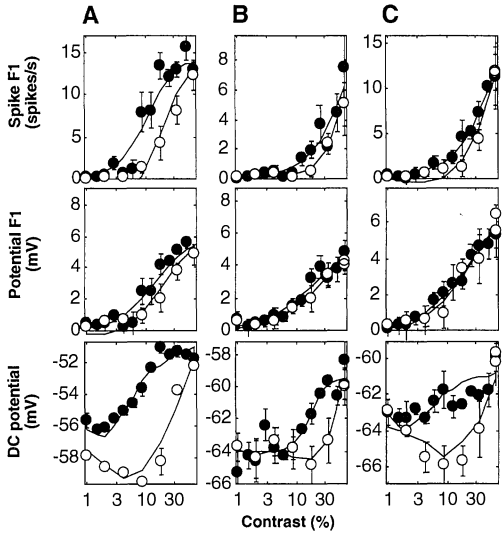

Fig. 3. Effects of contrast adaptation as measured with the ramp method (*13*). For three simple cells (**A** to **C**), the F1 component of the spike response (top), the F1 component of the membrane potential (middle), and the DC component of the membrane potential (bottom) are shown. The data in (A) are taken from the same cell as Fig. 1. Stimuli lasting 4 s were presented, the first at 1% contrast and each successive one at greater contrasts up to 64% (●). Contrast was then successively lowered back to 1% (○). The curves are fits of a model in which adaptation depends on the past responses of the cell. The adapted responses R_A are given by a hypothetical unadapted response R (described by Eq. 1) minus the sum of the five previous responses, each weighted by a factor that decayed exponentially in time:

$$R_A(t) = R(t) - k\sum_{s=1}^{5} \exp(-s/\tau)R_A(t-s) \quad (2)$$

The two parameters that describe adaptation are the strength, **K**, and the time constant, τ, of the exponential decay term. For each cell, τ was kept the same for all three fits. We use the parameter k to measure the strength of adaptation. Adaptation was always stronger in the DC potential than in the F1 potential, by a factor of 25 in (A), 4 in (B), 361 in (C), and 2 to 63 in the remaining six simple cells tested with ramps (median 9.3, $N = 9$). Although the model provided excellent fits to the ramp data, it would not account for the interleaved adaptation data because it predicts that the hyperpolarization induced by adaptation is the same for all test stimuli, which we know from Figs. 1 and 2 not to be the case.

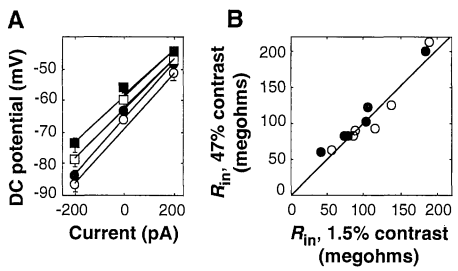

Fig. 4. Effects of adaptation on input resistance. (**A**) Current-voltage relation tested in one cell under four conditions. The contrasts of the test and adapting stimuli were 47% and 1.5% (■), 47% and 47% (□), 1.5% and 1.5% (●), and 1.5% and 47% (○). The ordinate is the DC component of the membrane potential recorded during a 4-s period of visual stimulation; the abscissa is the DC current injected through the recording electrode. Input resistance was measured as the inverse of the slope of the lines fitted to the data (least-squares fits). (**B**) Comparison of input resistance (R_{in}) measured in the two adaptation states. Each of six cells contributes two data points, one obtained while stimulating with 1.5% contrast gratings (●) and the other obtained while stimulating with 47% contrast gratings (○). The solid line fitted to the 12 points has slope 1.0 ± 0.003 and intercept 0.9 ± 0.3 megohm, indicating that adaptation was not associated with any noticeable change in input resistance.

R_{in} (Fig. 4A). The lines were displaced vertically from one another because the different test stimuli and adaptation states shifted the DC membrane potential. There was, however, little effect of visual stimulation (*22*, *23*) or adaptation on the slopes of the current-voltage relation, indicating that R_{in} changed little. This was true on average for all six cells tested; the linear fit through the points of Fig. 4B has a slope of unity and an intercept of <1 megohm, indicating no change in input resistance in the adapted state.

These measurements of R_{in} are more consistent with adaptation being caused by a decrease in tonic excitation than by an increase in tonic inhibition. Supporting evidence for a decrease in excitation underlying adaptation comes from in vitro experiments showing that intracortical synaptic excitation is depressed after repetitive electrical stimulation (*24*). Moreover, antagonists to presynaptic glutamate autoreceptors that mediate excitatory synaptic depression reduce extracellularly measured adaptation effects (*17*). GABA (γ-aminobutyric acid) antagonists, on the other hand, have little effect on adaptation (*17*, *18*). Taken together, these and our observations give strong support for the view that adaptation is caused by a decrease in the excitation received by a cell. In principle, this decrease could originate from an activity-dependent decrease in synaptic efficacy (*24*) whose effect would be enhanced if there were excitatory feedback among cortical cells (*25*). Our results provide the further constraint that adaptation must act largely through a tonic mechanism, which is an indicator of recent contrast history and operates both in the presence and in the absence of visual stimulation.

REFERENCES AND NOTES

1. L. Maffei, A. Fiorentini, S. Bisti, *Science* **182**, 1036 (1973); D. G. Albrecht, S. B. Farrar, D. B. Hamilton, *J. Physiol. (London)* **347**, 713 (1984).
2. R. G. Vautin and M. A. Berkeley, *J. Neurophysiol.* **40**, 1051 (1977).
3. J. A. Movshon and P. Lennie, *Nature* **278**, 850 (1979).
4. I. Ohzawa, G. Sclar, R. D. Freeman, *ibid.* **298**, 266 (1982); *J. Neurophysiol.* **54**, 651 (1985).
5. This phenomenon is uniquely cortical because it is essentially absent at earlier stages of visual processing (*4*) [T. Shou, X. Li, Y. Zhou, B. Hu, *Visual Neurosci.* **13**, 605 (1996)], and stimulation of one eye reduces the responses of cortical cells to stimulation of the other eye [L. Maffei, N. Berardi, S. Bisti, *J. Neurophysiol.* **55**, 966 (1986)].
6. H. B. Barlow, in *Vision: Coding and Efficiency*, C. Blakemore, Ed. (Cambridge Univ. Press, Cambridge, 1990); M. Carandini, H. B. Barlow, L. P. O'Keefe, A. B. Poirson, J. A. Movshon, *Philos. Trans. R. Soc. London Ser. B*, in press.
7. Whole-cell patch recordings in current clamp mode were obtained from barbiturate-anesthetized, paralyzed adult cats (*23*). Drifting sinusoidal gratings (mean luminance 15 cd/m^2) of optimal orientation, direction, spatial and temporal frequency, and window size were presented monocularly on an oscilloscope screen with an image generator (Innisfree, Cambridge, MA).
8. J. A. Movshon, I. D. Thompson, D. J. Tolhurst, *J. Physiol. (London)* **283**, 53 (1978).
9. D. G. Albrecht and D. B. Hamilton, *J. Neurophysiol.* **48**, 217 (1982).
10. This increase in the mean membrane potential with increasing contrast represents a nonlinearity in the responses of simple cells. We propose that it is caused by a differential contrast sensitivity of the excitatory and inhibitory inputs known to underlie the responses of simple cells (*12*). In this scenario, the responses at low contrasts are dominated by excitation, and inhibition appears only at higher contrasts. At low contrasts, increases in contrast cause increases in excitation that are relatively unopposed by increases in inhibition; as a result, the mean membrane potential increases with contrast. At higher contrasts, the inhibitory inputs begin to respond strongly, opposing the effects of increasing excitation and causing the mean potential to stop growing with contrast or even to decrease slightly.
11. C. Blakemore and F. W. Campbell, *J. Physiol. (London)* **203**, 237 (1969).
12. The depolarized portions of the visually driven membrane potential responses of a simple cell are attributable to increases in excitation as well as decreases in inhibition. Similarly, the hyperpolarized portions of these responses are attributable to decreases in excitation as well as increases in inhibition [D. Ferster, *J. Neurosci.* **8**, 1172 (1988)].
13. A. B. Bonds, *Visual Neurosci.* **6**, 239 (1991).
14. J. J. Kulikowski, V. M. Rao, T. R. Vidyasagar, *J. Physiol. (London)* **318**, 21P (1981); A. B. Saul and M. S. Cynader, *Visual Neurosci.* **2**, 593 (1989); S. Marlin, R. Douglas, M. Cynader, *J. Neurophysiol.* **69**, 2209 (1993).
15. J. A. Movshon, I. D. Thompson, D. J. Tolhurst, *J. Physiol. (London)* **283**, 79 (1978).
16. Other possible mechanisms include a long-lasting after-hyperpolarization [P. C. Schwindt *et al.*, *J. Neurophysiol.* **59**, 424 (1988)], an electrogenic pump, and a neuromodulatory effect on voltage-gated channels. Because adaptation could also be observed in the absence of spikes in the recorded cell, we doubt that the first mechanism is at work. It is doubtful that the second mechanism could produce hyperpolarizations as large as 15 mV. Our results, however, would be consistent with the third mechanism.
17. J. McLean and L. A. Palmer, *Visual Neurosci.* **13**, 1069 (1996).
18. E. J. DeBruyn and A. B. Bonds, *Brain Res.* **383**, 339 (1986); T. R. Vidyasagar, *Neuroscience* **36**, 175 (1990).
19. A. B. Saul, *Visual Neurosci.* **12**, 191 (1995).
20. R. S. Dealy and D. J. Tolhurst, *J. Physiol. (London)* **241**, 261 (1974); D. J. Heeger, *Visual Neurosci.* **9**, 181 (1992).
21. Assuming a passive neuron with a single compartment, the change in input resistance needed to hyperpolarize the membrane from V to V_A is $\Delta R_{in} = R_{in}(V_A - V)/(V - E_A)$, where E_A is the reversal potential of the synaptic input responsible for the hyperpolarization, and is 0 mV for excitatory postsynaptic potentials and –90 mV for inhibitory postsynaptic potentials. To produce a hyperpolarization from –65 to –70 mV, a decrease in excitation would require an 8% increase in R_{in}; an increase in inhibition would require a decrease of 20%. Simultaneous changes in excitation and inhibition could, of course, offset one another and result in a zero net change in R_{in}.
22. R. J. Douglas, K. A. C. Martin, D. Whitteridge, *Nature* **332**, 642 (1988).
23. D. Ferster and B. Jagadeesh, *J. Neurosci.* **12**, 1262 (1992).
24. S. B. Nelson, J. A. Varela, K. Sen, L. F. Abbott, in *The Neurobiology of Computation*, J. Bower, Ed. (Kluwer Academic, Boston, in press); E. V. Todorov, A. G. Siapas, D. C. Somers, S. B. Nelson, *ibid.*
25. R. J. Douglas, C. Koch, M. Mahowald, K. A. C. Martin, H. H. Suarez, *Science* **269**, 981 (1995).

26. We thank S. Chung for her contribution to the experiments and N. Spruston for his comments on the manuscript. Supported by National Eye Institute grant EY04726.

3 January 1997; accepted 18 March 1997

Regulation of Protein Phosphatase 2A by Direct Interaction with Casein Kinase 2α

Jean-Karim Hériché, Franck Lebrin, Thierry Rabilloud, Didier Leroy,* Edmond M. Chambaz, Yves Goldberg†

Timely deactivation of kinase cascades is crucial to the normal control of cell signaling and is partly accomplished by protein phosphatase 2A (PP2A). The catalytic (α) subunit of the serine-threonine kinase casein kinase 2 (CK2) bound to PP2A in vitro and in mitogen-starved cells; binding required the integrity of a sequence motif common to CK2α and SV40 small t antigen. Overexpression of CK2α resulted in deactivation of mitogen-activated protein kinase kinase (MEK) and suppression of cell growth. Moreover, CK2α inhibited the transforming activity of oncogenic Ras, but not that of constitutively activated MEK. Thus, CK2α may regulate the deactivation of the mitogen-activated protein kinase pathway.

Down-regulation of the mitogen-activated protein kinase (MAPK) cascade is crucial to normal growth control. PP2A plays an important role in this process by dephosphorylating the activating site in MAPK as well as in the enzyme that activates MAPK, MEK (MAPK or extracellular signal–regulated kinase kinase) (*1*). The core PP2A enzyme is a dimer of one catalytic (PP2Ac) and one regulatory (PR65/A) subunit; an additional, variable regulatory (B) subunit binds to PR65 and confers substrate specificity to the dephosphorylating activity (*2*). The SV40 virus–encoded small t antigen substitutes for one type of B subunit, resulting in a decrease in phosphatase activity toward MEK and an abnormal activation of the mitogenic MAPK cascade (*3*).

CK2 is a widely expressed, conserved serine-threonine kinase, the signaling function of which is obscure (*4*). Holoenzymic CK2 is a constitutively active tetramer of